Supporting Information

Dynamic Disorder in Single Enzyme Reactions: Facts and Artifacts

Tatyana G. Terentyeva, Hans Engelkamp, Alan E. Rowan, Tamiki Komatsuzaki*, Johan Hofkens*, Chun-Biu Li* and Kerstin Blank*

*To whom correspondence should be addressed.

tamiki@es.hokudai.ac.jp

Johan.Hofkens@chem.kuleuven.be

cbli@es.hokudai.ac.jp

K.Blank@science.ru.nl

1. Generation of the photon arrival time sequence

A state sequence was first produced by performing a random walk in the kinetic scheme (as a Markov model, see Fig. 1) with the corresponding state-to-state transition probabilities given by the rate constants listed in table S1. The chosen time step (10 μs) of the random walk was much smaller than the time scales specified by all the rates. The random state sequence was then translated into an on/off sequence according the on- (and off-) state assignment in Fig. 1.

Table S1. Rate constants used to simulate the on/off dwell time series; units: s^{-1}

	conformational change			catalytic reaction				
	α	β	γ	k_{1a} k_{1b}	k_{-1a} k_{-1b}	k_{2a} k_{2b}	$k_{2a'}$ $k_{2b'}$	k_{3a} k_{3b}
model 1	5×10^{2}	7.5×10^{2}	6×10^{2}	7.5×10^{2} 3×10^{2}	1×10^{2} 1.5×10^{2}	4×10^{1} 1×10^{1}	3×10^{2} 1×10^{2}	5×10^{4} 5×10^{4}
model 2	5×10^{0}	0.5×10^{0}	6×10^{0}	7.5×10^{3} 3×10^{3}	1×10^{2} 1.5×10^{2}	4×10^{1} 1×10^{1}	3×10^{2} 1×10^{2}	5×10^{4} 5×10^{4}

The “on”/”off” time sequences for both models were validated by determining the “on” and “off” dwell time histograms and comparing them to the distributions calculated from the Markov model (Fig. S1).

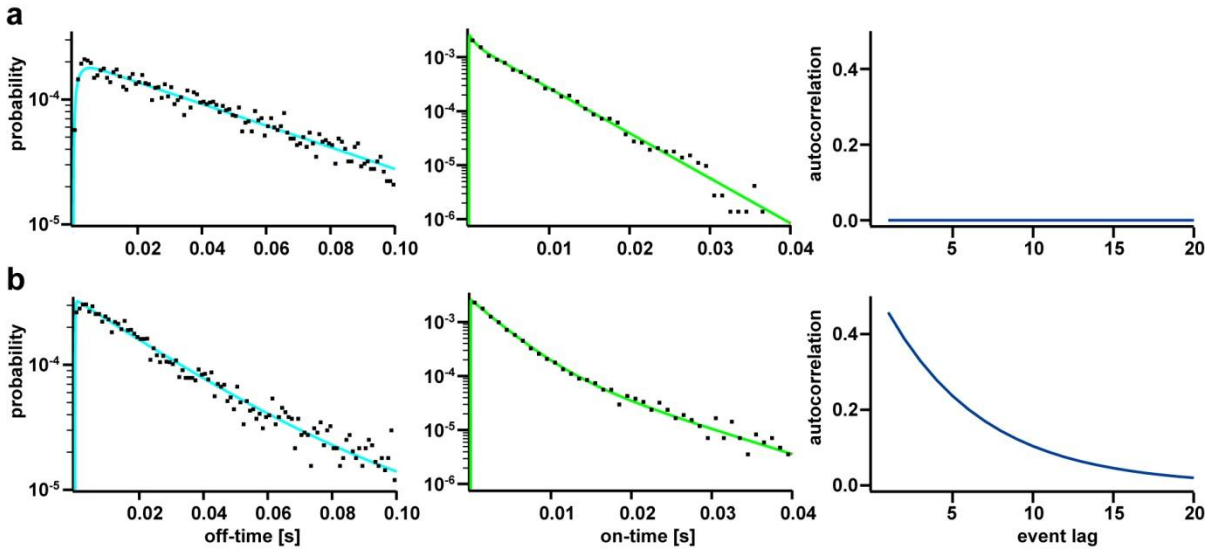

Figure S1. Expected results for model 1 (a) and model 2 (b). The solid lines represent the underlying off-time histogram (cyan), on-time histogram (green) and the autocorrelation plot of the off-times (blue). The black dots represent the dwell time histograms obtained after analyzing the simulated on-off time series (before the addition of Poisson noise).

In the next step, an intensity time series $I(t)$ was obtained for different "on" and "off" intensity levels (table S2). The corresponding photon train, a series of inter-photon times (τ_1, τ_2, τ_3,…), was generated from $I(t)$ according to Poisson statistics, *i.e.*, the probability to observe the inter-photon time between (τ, $\tau + d\tau$) for a given intensity I is given by $P(\tau|I) = I \exp(-I\tau)\, d\tau$.

Table S2. Intensity levels for the signal and the background levels used to simulate the photon arrival time sequences; units: photons/s

	background intensity			
	2000	4000	6000	8000
S:N = 1.5:1	3000	6000	9000	12000
S:N = 2.5:1	5000	10000	15000	20000
S:N = 3.5:1	7000	14000	21000	28000

S:N = 4.5:1	9000	18000	27000	36000

2. Change point analysis of the simulated photon arrival time sequence

The assignment of the “on”/”off” levels from the time-resolved single molecule emission trajectory is usually performed by binning/thresholding methods. The photon arrival time trace is first binned to obtain an intensity trace and then a threshold is applied to discriminate “on” and “off” (see Fig. S2a).

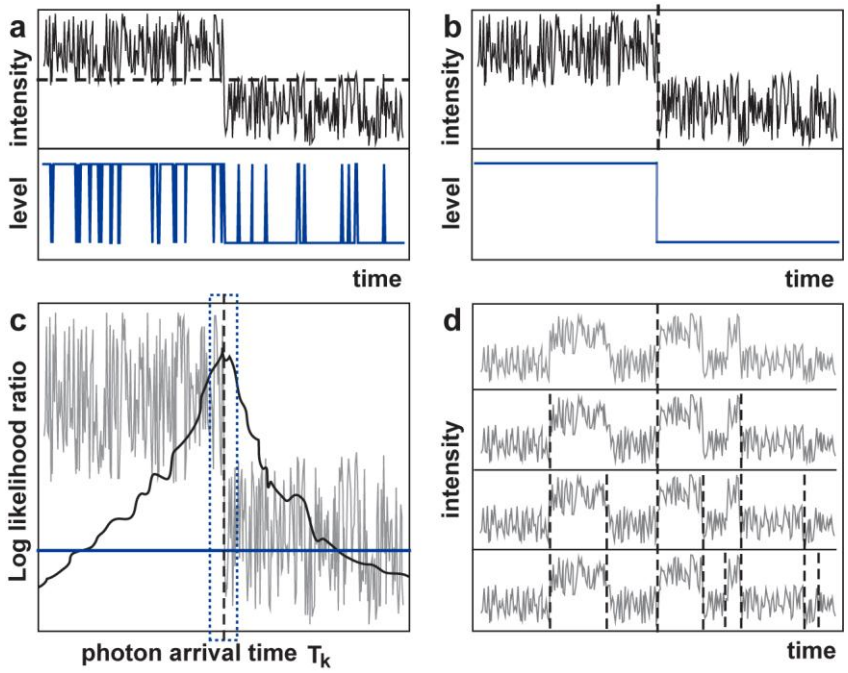

Figure S2. Principle of change point analysis. (a)-(b) Intuitive comparison of thresholding and change point methods. (c) The LLR of the two hypotheses: change point exists at the *k*th photon located at time T_k (H_A), and the *k*th photon is not a change point (H_0). The lower blue line is the critical value of the LLR above which a change point likely exists with the change point most likely located at the maximum of the LLR (dashed line). The location uncertainty of the change point (blue dotted box) can also be estimated. The intensity time trace obtained with binning is shown in gray for comparison. (d) Multiple change points are detected by applying the LLR test recursively thereby binary segmenting the photon arrival time trace. The dashed lines show the location of the most likely positions of the change points.

It is evident from Fig. S2a and the discussion in the main text that the assignment of “on” and “off” levels becomes problematic when the signal-to-noise (S:N) ratio is low. In

particular, false and rapid switches between the “on” and “off” levels can occur leading to the overestimation of events in the dwell time distribution and artificial correlations in the short off-time region. This problem can be resolved by the detection of intensity change points as shown schematically in Fig. S2b. Below the main concepts and procedures of the change point detection developed by Watkins *et al*.[1] and employed in this work are summarized.

2.1. Change point detection as a hypothesis test

Following Watkins *et al*.,[1] the detection of an intensity change point for a given photon arrival time trace is treated as a hypothesis test problem. We compare statistically the following two hypotheses for each photon in the trace: a) the photon under consideration is not a change point (called the null hypothesis and denoted by H_0); b) the photon under consideration is a change point (called the alternative hypothesis and denoted by H_A). To compare the statistical significance of the two hypotheses, we consider the log likelihood ratio (LLR) of the two hypotheses for the *k*th photon in the photon trace:

$$L(k) = \ln \frac{P(H_A|k)}{P(H_0|k)} \tag{1}$$

where $P(H_A|k)$ and $P(H_0|k)$ are the probabilities (or likelihoods) for the hypothesis H_A and H_0 for the *k*th photon, respectively. In other words, the *k*th photon is more likely to be an intensity change point if *L(k)* is large. On the other hand, since the probability of observing *n* photons for a given intensity *I* and duration *T* is given by the Poisson distribution

$$g(n|I,T) = \frac{(IT)^n e^{-IT}}{n!} \tag{2}$$

the likelihoods $P(H_A|k)$ and $P(H_0|k)$ can then be expressed as

$$P(H_A|k) = g(k|I_1 = \frac{k}{T_k}, T_k)g(N-k|I_2 = \frac{N-k}{T-T_k}, T-T_k)$$
$$P(H_0|k) = g(k|I_0 = \frac{N}{T}, T_k)g(N-k|I_0 = \frac{N}{T}, T-T_k) \quad (3)$$

where T_k, N and T are the photon arrival time of the kth photon (with the first photon arriving at $T_1 = 0$), the total number of photons in the trace and the total time length of the trace, respectively. I_0, I_1 and I_2 are the estimated intensities of the whole trace, the part of the trace preceding the kth photon and the part succeeding the kth photon, respectively. Eq. 3 distinguishes H_A and H_0 by imposing the change of intensity from I_1 to I_2 if the kth photon is an intensity change point. The intensity remains to be I_0 if the kth photon is not a change point. Fig. S2c shows an example of the LLR (Eq. 1) evaluated for each photon in a photon train. The LLR peaks at the most likely position for the occurrence of an intensity change (shown by the dashed line in Fig. S2c). The photon located at this peak value is assigned as an intensity change point if its LLR value is larger than a critical value (indicated by the blue line in Fig. S2c) calculated using a recursive algorithm of Noé.[2] It is concluded that no change point exists if the LLR is smaller than the critical value in the whole photon train under consideration.

It is noted that the above scheme for identifying intensity change points is based on a photon-by-photon LLR hypothesis test. Therefore, the time resolution in locating the change point is limited by the inter-photon time. In contrast, in the case of thresholding methods the accuracy of the change point location is limited by the choice of the bin size in the intensity trace. Other change point detection schemes using Bayesian approaches based on a hypothesis test have also been proposed.[3,4] The main difference between these and the method by Watkins *et al*.[1] is the way how the hypotheses are compared statistically. The hypothesis test scheme proposed by Watkins *et al*.[1] is chosen in this work as it has performed better practically in identifying change points in our simulated data

even in low S:N cases. A detailed comparison of the performance of these methods will be discussed elsewhere.

2.2. Multiple change point detection

To identify multiple change points in the photon arrival time trace, we have applied the above scheme recursively by binary segmentation. Fig. S2d schematically shows the procedure for locating multiple change points. For a given photon trace, we first applied the LLR hypothesis test to decide if a change point exists and to locate the most likely photon as the change point (top panel of Fig. S2d). The photon trace was then divided into two disjoint segments separated by the change point just found. The LLR hypothesis test was applied again to each of the segments to identify additional change points (second panel of Fig. S2d). The binary segmentation was then repeated (third and forth panel of Fig. S2d) until no change points could be found in the segments anymore.

2.3. Assignment of "on" and "off" intensity levels

In practice, the application of the above multiple change point detection procedure will result in more change points as expected. This is illustrated in Fig. S3a where the dashed lines denote the change points detected with the above method. Intuitively, one would expect that the "on"/"off" level assignment should look like the example given in Fig. S3c. The appearance of redundant change points in Fig. S3a can be caused by several experimental factors, such as fluctuations in the background intensity (giving rise to the extra change points separating the change point intervals 8, 9 and 10 in Fig. S3a), the non-uniformity of the excitation intensity in the detection volume and the existence of multiple intensity levels of the fluorescent product (which give rise to the extra change point separating the change point intervals 2 and 3 in Fig. S3a), *etc*.

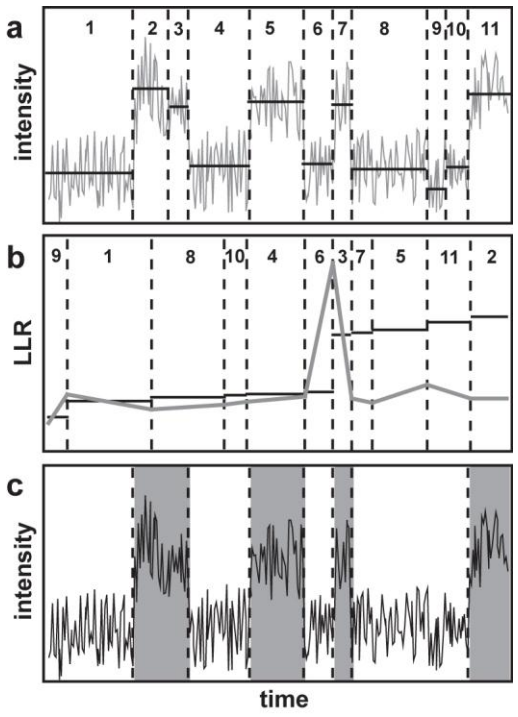

Figure S3. Change point cleanup procedure. (a) Undesired change points may result from some unknown experimental factors and need to be removed to accurately assign the "on" and "off" levels to the intervals between two change points. The intervals are labeled with numbers for easy comparison. (b) Sorting of the change point intervals by their estimated intensities and the corresponding calculated LLR (Eq. 1) locating the most significant intensity change. The black lines denote the estimated intensities (number of photons/time) for each change point interval. The gray line denotes the LLR. All change point intervals left from the maximum LLR are assigned to be "off" and those to the right are assigned to be "on". (c) The consecutive "on"/"off" change point intervals are concatenated together. The gray (white) areas represent the "on" ("off") levels.

In most cases the amplitudes of these undesired fluctuations are small compared to the intensity changes originating from the conversion of the fluorogenic substrate into the fluorescent product. Based on this assumption the following cleanup procedure can be applied to remove the extra change points:

1) In order to deal with the possibility of slow intensity fluctuations at the background (noise), we have chosen a set (or window) of consecutive change point intervals (*e.g.* the set shown in Fig. S3a).
2) The change point intervals in this set were then sorted in ascending order according to the estimated intensity of the change point intervals (see Fig. S3b). The estimated intensity of a change point interval is simply equal to the number of photons in the interval divided by the duration of the interval.

3) Next, the LLR (Eq. 1) was evaluated for each of the change points in the sorted set as shown by the gray line in Fig. S3b. The change point at which the LLR reaches its maximum (*e.g.* the change point separating intervals 6 and 3 in Fig. S3b) signifies the largest intensity change in the set and, therefore, serves as a separation point between the "off" and "on" levels. All change point intervals placed to the left from this separation point were assigned as belonging to the "off" level and those to the right were assigned as belonging to the "on" level.
4) Finally, consecutive "on" and "off" change point intervals were concatenated together to obtain the on/off assignments as shown in Fig. S3c. The above procedure was then repeated for the other disjoint sets (or windows) of change point intervals of the trace. For the analysis of the experimental data the window size was chosen such that each window contained around 100 change point intervals. It was found that the resulting statistics of the on/off dwell times is not sensitive to this number, as long as the number is neither too small nor too large.

We note that the second operation of change point analysis discussed above can be generalized for systems with more than two levels, *e.g.* in ion channel gating and quantum dot blinking. In such cases, the number of underlying levels in the system can be determined from the number of significant LLR maxima in Fig. S3b provided that the undesired fluctuations at each level are small compared to the intensity changes at the level-to-level transitions.

3. Discussion of the results of the binning/thresholding analysis of model 2

3.1. Influence of the bin size

The graphs in Fig. 3a show the influence of the bin size on both the off- and on-histogram for the data set with a S:N ratio of 10000:4000 photons/s. A clear influence can be seen and only the smallest bin size of 1 ms yields off- and on-histograms that have a similar slope as the underlying histograms.

When looking at the other 15 simulated data sets it becomes evident that it is not possible to use a bin size of 1 ms for the data sets with low S:N ratios and/or low intensity levels as the number of photons/bin is too low. In these cases the smallest bin size used was 2.5 ms (see table S3 for the bin sizes used). In none of these cases a good match between the analysis results and the underlying histograms could be obtained. For the data sets where a bin size of 1 ms could be applied the signal and background intensity distributions overlap by less than 50% if the S:N ratio is at least 2.5 and the background intensity level is higher than 4000 photons/s. Only in these cases a separation between the two distributions is visible (*vide infra*) and a threshold value can be assigned unambiguously.

The result that only the smallest possible bin size yields the expected result has two experimental consequences. i) When a CCD camera is used for detection for the fluorescent signal the on- and off-time distributions are only meaningful when measured with a very good time resolution (ideally 1 ms) and for many applications CCD detection might not be useful. ii) Choosing a bin size long enough to yield a good separation between the signal and the background intensity distribution may lead to an inappropriate analysis result. In all our data sets, the larger bin sizes lead to a better separation of the intensity distributions but to a less accurate analysis result. The bin size needs to be as small as possible. In our analysis we therefore used a bin size of 1 ms whenever possible.

3.2. Influence of the threshold method

For the analysis 3 different threshold methods have been used. Methods A and B are very similar. In both methods the threshold is placed at the intersection between the signal and the background intensity distribution. For method A a correction was used that we call “interpeak time” correction in the following. With this correction, on-times, separated by only one “off”-bin (or several “off”-bins within this interpeak time), were counted as only one on-time. This correction can account for noise in the on-state that might fluctuate around the threshold value (a problem that might occur especially in data with low S:N ratios; Fig. 2). In method C the threshold was set at a position ensuring that less than 5% of the “off”-bins were counted as “on”-bins.

Threshold C was always lower than thresholds A and B. As a result, the number of on-times obtained with method C was always higher than with the other methods. When comparing the number of on-times with the expected number of turnovers, method C overestimates this number to the largest extent (see table S3). Also the shapes of the off- and on-histograms do not match the underlying ones (Fig. 3a). As method C can further not be applied to data where the signal and the background intensity distributions are separated (*i.e.* the data sets with good S:N ratios) we conclude that method C is not useful. A comparison of methods A and B for the data set with a S:N ratio of 10000:4000 photons/s shows that both methods detect a higher number of short off-times as is expected from the underlying histogram (Fig. 3b). The off-histogram closest to the underlying one is obtained for method A with an interpeak time of 5 ms. It can be clearly seen that the use of the interpeak time correction influences the analysis result and that method B without the interpeak time correction detects the highest number of short off-times. This is a clear indication that fluctuations in the on-state do lead to an artificial separation of one on-state into several shorter on- and off-states. This segmentation of on-states is also responsible for the overestimation of the number of short on-times.

Although the use of this correction seems to improve the analysis result it also introduces another subjective factor into the analysis. In the simulated data set the average on-time is around 5 ms. Consequently, choosing an interpeak time of 5 ms will lead to the correct result. In experimental data, however, the duration of the on-time is not known *a priori* and on-times might be combined artificially. Truly short off-states would then be discarded. The usefulness of the interpeak time correction will further depend on the bin size one may choose. For bin sizes larger than 1 ms, intensity fluctuations will be averaged out within the bin and the influence of the correction might be minimal. In our analysis we have used a correction setting the interpeak time such that only single “off”-bins will be combined with the on-time. The analysis of the other 15 data sets with methods A and B show the same overall tendency. The difference between methods A and B is becoming smaller for increasing S:N ratios.

From an experimental point of view, the performance of threshold analysis can only be improved with better S:N ratios and to some extent also with a higher overall intensity (*vide infra*). For data with a bad S:N ratio it might not even be possible to identify the intersection between the intensity distributions and another less accurate approach similar to method C might have to be used.

3.3. Influence of the S:N ratio

Having established that a bin size of 1 ms and threshold method A are the best approach for our data, the influence of the S:N ratio was analyzed next (Fig. 3c). Except for the very low S:N ratio of 1.5 all off-histograms reproduced the overall shape of the underlying histogram fairly well. For the 2.5, 3.5 and 4.5 S:N ratios the only difference was in the number of short off-times that was again higher as for the underlying distribution. Most importantly, this number was highest for the lowest S:N ratio and decreased for the higher S:N ratios. For S:N of 3.5 and 4.5 also the on-histograms resembled the underlying

histogram rather well. This result is expected as for better S:N ratios the background and signal intensity levels are more clearly separated and the probability of segmenting on-times is reduced. (The S:N ratio is probably the parameter which is the most difficult to optimize in an experimental setting as it is limited by the photon emission rate of the fluorescent dye and the intrinsic background of the measurement.)

3.4. Influence of the intensity level

Using a bin size of 1 ms and threshold method A, we also observed an improvement in both the off- and on-histograms with an increase in the overall intensity (Fig. 3d). Even for the S:N ratio of 2.5 shown in Fig. 3d, an increase in the total number of photons lead to an improvement of the analysis and for the highest intensity level (20000:8000 photons/s) both the off- and the on-histograms were reproduced very well. This means that, even when the S:N ratio cannot be improved, an increase in the overall intensity can improve the accuracy of the analysis. Experimentally this may, for example, be achieved by increasing the laser intensity.

4. Comparison of the results for model 1

Identical data sets have been generated for model 1 and analyzed with threshold method A (2 ms interpeak time) and change point analysis. Two representative off-histograms and the corresponding on-histograms are shown in Fig. S4.

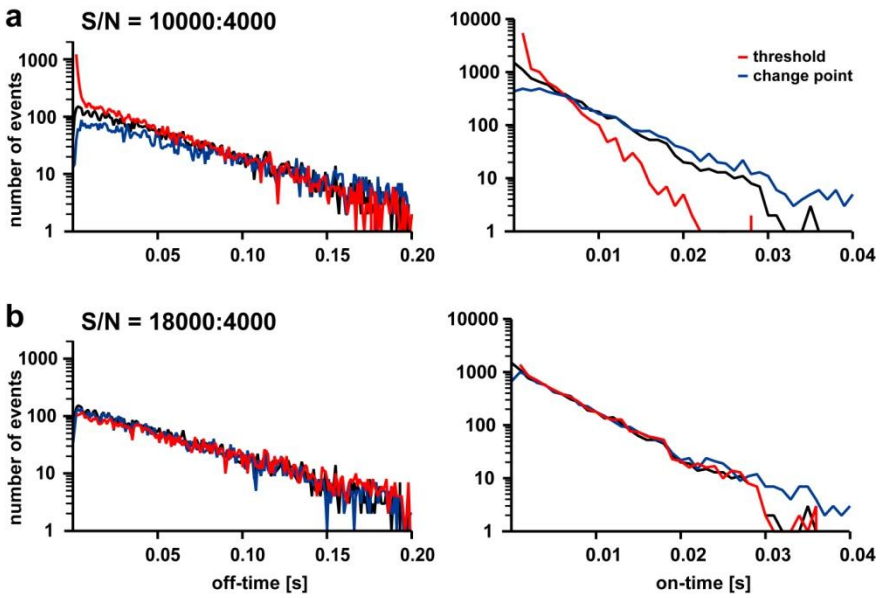

Figure S4. Off- and on-histograms for two data sets of model 1. For (a) the S:N ratio was 10000:4000 photons/s and for (b) 18000:4000 photons/s. The black lines represent the underlying on- and off-histograms. For the threshold analysis method A with 2 ms interpeak time was used.

The off-histograms for the S:N ratio of 10000:4000 photons/s again did not match the underlying histogram and showed deviations in the short off-time region. Most importantly, the binning/thresholding approach failed to capture the maximum in the short off-time region (see black line in Fig. S4a) and again yielded a larger number of short off-times as expected. Although the underlying histograms are very different for model 1 and 2 in the short off-time region, histograms with the same overall shape were obtained for both models with threshold analysis. Also with change point analysis the histograms for model 1 and 2 were very similar in shape. This shows very clearly that the shape of the histogram

in the short off-time region is not determined by the underlying kinetic scheme but by the errors in the data analysis procedure.

For the S:N ratio of 10000:4000 photons/s the on-histogram was also not reproduced accurately with both methods, although change point analysis performed much better. Also in this case the artificial segmentation of on-states with the threshold method lead to an overestimation of short on-times and an underestimation of long on-times. For the higher S:N ratio (18000:4000 photons/s) the accuracy was much better and the slope for the long on-times was reproduced very well with both analysis methods.

5. Determination of false positive and false negative events

In order to establish additional parameters to describe the accuracy of the binning/thresholding and the change point approach the number of not accurately detected on-times (false-positive and false-negative events) was quantified according to the procedure in Fig. S5. The simulated “on”/”off” time series and the time series after analysis were both binned with a bin size of 1 ms. This bin size is on a similar time scale as the average on-time and much smaller than the average off-time. In this way, each on-event is ideally located into one bin separated by several empty bins so that each bin contains either no event or one event. In the next step the two binned traces are subtracted from each other. If the expected and the detected on-events are located in the same bin the resulting value will be “0” (meaning that the event has been detected correctly). In cases where an on-time was detected wrongly the resulting trace will either contain +1 or -1 at the respective positions. The total number of “+1” yields the number of false-positives and the total number of “-1” yields the number of false-negatives. The results are summarized in table S4.

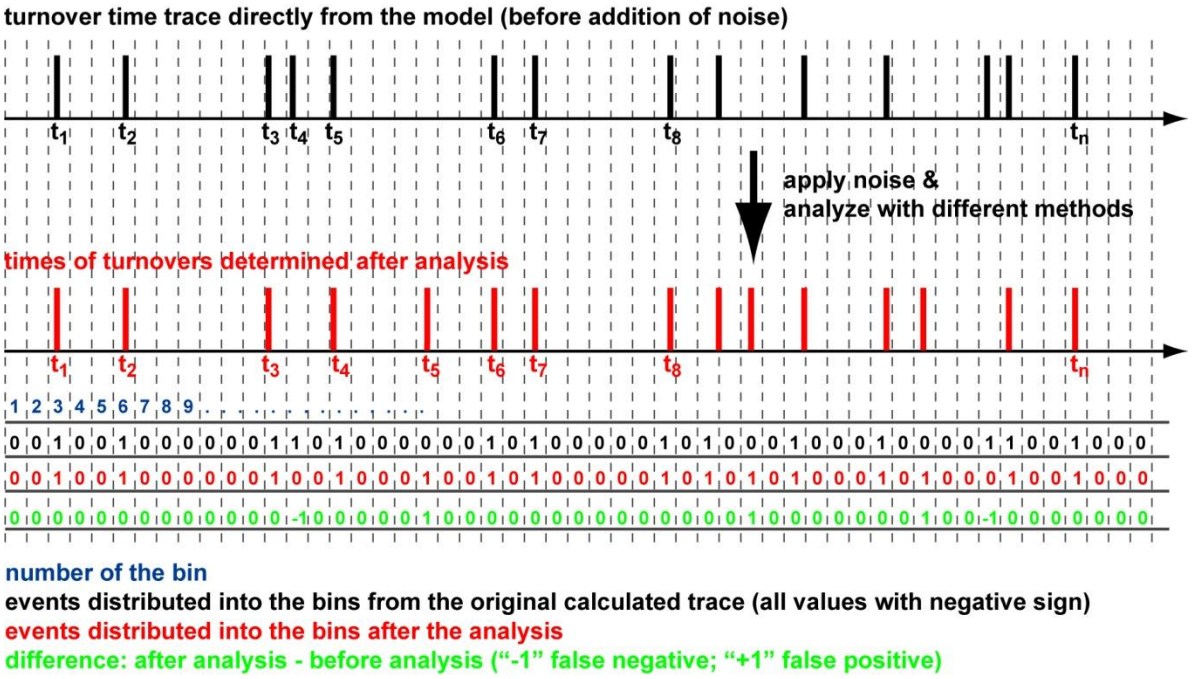

number of the bin
events distributed into the bins from the original calculated trace (all values with negative sign)
events distributed into the bins after the analysis
difference: after analysis - before analysis ("-1" false negative; "+1" false positive)

Figure S5. Determination of false-positive and false-negative events. False-positive is defined as an off-event detected as an additional on-event (*e.g.* t_5 in the lower trace) and false-negative is defined as an on-time which was missed by the analysis procedure (*e.g.* t_4 in the upper trace).

References

(1) Watkins, L. P.; Yang, H. Detection of Intensity Change Points in Time-Resolved Single-Molecule Measurements. *J. Phys. Chem. B* **2005,** *109*, 617-628.

(2) Noé, M. The Calculation of Distributions of Two-Sided Kolmogorov-Smirnov Type Statistics. *Ann. Math. Stat.* **1972,** *43*, 58-64.

(3) Kalafut, B.; Visscher, K. An Objective, Model-Independent Method for Detection of Non-Uniform Steps in Noisy Signals. *Comput. Phys. Commun.* **2008,** *179*, 716-723.

(4) Ensign, D. L.; Pande, V. S. Bayesian Detection of Intensity Changes in Single Molecule and Molecular Dynamics Trajectories. *J. Phys. Chem. B* **2010,** *114*, 280-292.

Table S3. Summary of the mean off-time (<t_{off}>), the mean on-time (<t_{on}>) and the total number of turnovers (TO)

noise, hv/s	signal ,hv/s	bin, ms	<t_{off}>^{A}, ms	<t_{off}>^{B}, ms	<t_{off}>^{C}, ms	<t_{off}>^{D}, ms	<t_{on}>^{A}, ms	<t_{on}>^{B}, ms	<t_{on}>^{C}, ms	<t_{on}>^{D}, ms	TO^{A}	TO^{B}	TO^{C}	TO^{D}
2000	3000	2.5 5 10	0.029 0.235 0.296	0.026 0.225 0.283	0.048 0.057 0.117	0.240	0.0036 0.0058 0.0120	0.0029 0.0053 0.0111	0.0027 0.0059 0.0119	0.2042	12186 1663 1300	13810 1737 1358	7805 6371 3093	901
2000	5000	2.5 5 10	0.145 0.106 0.168	0.129 0.099 0.157	0.035 0.044 n.d.	0.092	0.0038 0.0094 0.0159	0.0031 0.0084 0.0142	0.0049 0.0081 n.d.	0.0218	2682 3459 2179	3022 3735 2333	10286 7743 n.d.	3523
2000	7000	1 2.5 5	0.041 0.072 0.101	0.03 0.066 0.095	0.022 0.044 n.d.	0.067	0.0029 0.0069 0.0103	0.0018 0.006 0.0093	0.0020 0.0052 n.d.	0.0127	9076 5063 3595	12611 5580 3827	16873 10314 n.d.	4997
2000	9000	1 2.5 5	0.044 0.070 0.084	0.033 0.067 0.078	0.025 n.d. n.d.	0.058	0.0043 0.0073 0.0109	0.0028 0.0068 0.0096	0.0028 n.d. n.d.	0.0105	8249 5163 4203	11303 5440 4550	14582 n.d. n.d.	5849
4000	6000	2.5 5 10	0.182 0.111 0.178	0.173 0.102 0.165	0.030 0.060 0.084	0.127	0.0030 0.0053 0.0144	0.0027 0.0061 0.0126	0.0030 0.0064 0.0132	0.0748	2167 3375 2083	2280 3708 2254	12214 6013 4117	1981
4000	10000	1 2.5 5	0.034 0.067 0.100	0.025 0.06 0.095	0.019 0.026 n.d.	0.058	0.0026 0.0067 0.0100	0.0017 0.0057 0.0092	0.0018 0.0048 n.d.	0.0136	10896 5423 3610	14644 6085 3832	19459 12902 n.d.	5569
4000	14000	1 2.5 5	0.047 0.066 0.088	0.035 0.063 0.074	0.022 n.d. n.d.	0.049	0.0056 0.0074 0.0098	0.0032 0.0069 0.0097	0.0029 n.d. n.d.	0.0093	7753 5453 4383	10355 5727 4757	15770 n.d. n.d.	6865
4000	18000	1 2.5 5	0.051 0.060 0.072	0.046 0.057 0.066	n.d. n.d. n.d.	0.046	0.0054 0.0077 0.0116	0.0047 0.0071 0.01	n.d. n.d. n.d.	0.0084	7052 5909 4793	7896 6260 5277	n.d. n.d. n.d.	7392
underlying true values			**<t_{off}> = 0.043**				**<t_{on}> = 0.0047**				**TO = 8395**			

[A]Threshold method A (cut-off at intersection, interpeak correction); [B]Threshold method B (cut-off at intersection, no interpeak correction), [C]Threshold method C (less than 5% false positive “on”-bins), [D]Change point analysis

Table S3 (continued). Summary of the mean off-time (<t_{off}>), the mean on-time (<t_{on}>) and the total number of turnovers (TO)

noise, hv/s	signal ,hv/s	bin, ms	<t_{off}>^{A}, ms	<t_{off}>^{B}, ms	<t_{off}>^{C}, ms	<t_{off}>^{D}, ms	<t_{on}>^{A}, ms	<t_{on}>^{B}, ms	<t_{on}>^{C}, ms	<t_{on}>^{D}, ms	TO^{A}	TO^{B}	TO^{C}	TO^{D}
6000	9000	2.5 5 10	0.073 0.108 0.171	0.065 0.09 0.161	0.035 0.045 0.068	0.088	0.0037 0.0081 0.0149	0.0031 0.0068 0.0134	0.0033 0.0071 0.0140	0.0473	5239 3460 2152	5880 3827 2291	10433 7609 4895	2950
6000	15000	1 2.5 5	0.042 0.071 0.092	0.029 0.066 0.086	0.014 0.031 n.d.	0.048	0.0035 0.0072 0.0104	0.0021 0.0065 0.0094	0.0020 0.0052 n.d.	0.0111	8823 5128 3912	12706 5517 4181	24454 11142 n.d.	6798
6000	21000	1 2.5 5	0.049 0.064 0.074	0.043 0.062 0.068	0.015 n.d. n.d.	0.042	0.0052 0.0075 0.0110	0.0044 0.007 0.01	0.0026 n.d. n.d.	0.0084	7311 5548 4694	8400 5834 5148	22521 n.d. n.d.	7911
6000	27000	1 2.5 5	0.051 0.060 0.068	0.049 0.056 0.061	n.d. n.d. n.d.	0.040	0.0056 0.0078 0.0121	0.0054 0.0067 0.0103	n.d. n.d. n.d.	0.0082	7097 5920 4995	7333 6277 5588	n.d. n.d. n.d.	8302
8000	12000	2.5 5 10	0.061 0.095 0.157	0.053 0.088 0.146	0.033 0.048 n.d.	0.071	0.0043 0.0086 0.0155	0.0034 0.0075 0.0137	0.0035 0.0075 n.d.	0.0330	6120 3849 2320	7058 4198 2498	11063 7259 n.d.	3861
8000	20000	1 2.5 5	0.044 0.066 0.078	0.032 0.063 0.072	0.017 n.d. n.d.	0.042	0.0043 0.0073 0.0109	0.0028 0.0068 0.0097	0.0025 n.d. n.d.	0.0100	8289 5429 4522	11371 5716 4909	20752 n.d. n.d.	7616
8000	28000	1 2.5 5	0.051 0.059 0.067	0.048 0.056 0.061	n.d. n.d. n.d.	0.039	0.0055 0.0077 0.0121	0.0051 0.0071 0.0103	n.d. n.d. n.d.	0.0083	7071 5977 5037	7568 6345 5600	n.d. n.d. n.d.	8544
8000	36000	1 2.5 5	0.052 0.056 0.063	0.05 0.052 0.056	n.d. n.d. n.d.	0.036	0.0057 0.0080 0.0126	0.0056 0.0073 0.0106	n.d. n.d. n.d.	0.0079	6981 6280 5303	7160 6702 5988	n.d. n.d. n.d.	9056
underlying true values			**<t_{off}> = 0.043**			**<t_{on}> = 0.0047**			**TO = 8395**					

^{A}Threshold method A (cut-off at intersection, interpeak correction); ^{B}Threshold method B (cut-off at intersection, no interpeak correction), ^{C}Threshold method C (less than 5% false positive “on”-bins), ^{D}Change point analysis

Table S4. Number of on-events detected as off-events (false -) and off-events detected as on-events (false +) for the best threshold method (A, cut-off at intersection, interpeak correction) and when using change point analysis (D)

noise	2000	2000	2000	2000	4000	4000	4000	4000	6000	6000	6000	6000	8000	8000	8000	8000
signal	3000	5000	7000	9000	6000	10000	14000	18000	9000	15000	21000	28000	12000	20000	28000	36000
bin[1], ms	5	5	2.5	1	5	1	1	1	2.5	1	1	1	2.5	1	1	1
A: false -	8230	7788	6740	5593	8027	5858	5292	5271	7651	5526	5141	5461	7408	5122	5198	5409
A: false +	1507	2861	3417	5456	3017	8369	4654	3937	4504	5963	4070	4173	5142	5025	3883	4004
A: sum	9737	10649	10157	11049	11044	14227	9946	9208	12008	11489	9211	9634	12550	10147	9081	9413
D: false -	8279	8302	5534	4434	8050	5998	3744	2894	7783	4638	3580	2162	7508	3889	2349	1846
D: false +	795	3445	2146	1898	1646	3182	2224	1901	2348	3051	3106	2079	2984	3120	2508	2517
D: sum	9074	11747	7680	6332	9696	9180	5968	4795	10131	7689	6686	4241	10492	7009	4857	4363

[1]Only data for the smallest analyzable bin size is shown in the table.